Annals of Biomedical Engineering, Vol. 33, No. 4, April 2005 (© 2005) pp. 429–443
DOI: 10.1007/s10439-005-2498-z

A Comparison of Flow Field Structures of Two Tri-Leaflet Polymeric Heart Valves

HWA-LIANG LEO,[1,2] HÉLÈNE SIMON,[3] JOSIE CARBERRY,[1] SHAO-CHIEN LEE,[3] and AJIT P YOGANATHAN[1]

[1]Wallace H. Coulter School of Biomedical Engineering, Georgia Institute of Technology, Atlanta, GA; [2]Woodruff School of Mechanical Engineering, Georgia Institute of Technology, Atlanta, GA; and [3]School of Chemical and Biomolecular Engineering, Georgia Institute of Technology, Atlanta, GA

(Received 30 March 2004; accepted 18 October 2004)

Abstract—Polymeric heart valves have the potential to reduce thrombogenic complications associated with current mechanical valves and overcome fatigue-related problems experienced by bioprosthetic valves. In this *in vitro* study, the velocity fields inside and downstream of two different prototype tri-lealfet polymeric heart valves were studied. Experiments were conducted on two 23 mm prototype polymeric valves, provided by AorTech Europe, having open or closed commissure designs and leaflet thickness of 120 and 80 μm, respectively. A two-dimensional LDV system was used to measure the velocity fields in the vicinity of the two valves under simulated physiological conditions. Both commissural design and leaflet thickness were found to affect the flow characteristics. In particular, very high levels of Reynolds shear stress of 13,000 dynes/cm^2 were found in the leakage flow of the open commisure design. Maximum leakage velocities in the open and closed designs were 3.6 m/s and 0.5 m/s respectively; the peak forward flow velocities were 2.0 m/s and 2.6 m/s, respectively. In both valve designs, shear stress levels exceeding 4,000 dyne/cm^2 were observed at the trailing edge of the leaflets and in the leakage and central orifice jets during peak systole. Additionally, regions of low velocity flow conducive to thrombus formation were observed in diastole. The flow structures measured in these experiments are consistent with the location of thrombus formation observed in preliminary animal experiments.

Keywords—Fluid mechanics, Polyurethanes, Coaptation, Washout, Vena contracta, Gap channel, Oscillation.

INTRODUCTION

Currently, mechanical prosthetic valves are the most widely implanted heart valve prostheses. Despite their superior hemodynamic properties and durability, the present mechanical prostheses are still prone to thromboembolic complications causing patients to require lifelong anti-coagulation therapy.[12,27] Bioprosthetic valves, which are largely porcine in origin, are an alternative to the mechanical prostheses. The tissue based valves exhibit good hemodynamic performance, however they are especially prone to calcification and tissue failure.[21,25]

The tri-leaflet polymeric heart valve attempts to mimic the geometry of the native valve while maintaining the durability of the current mechanical prostheses. This valve, which is currently under development, is expected to reduce or prevent thrombosis related complications,[28] thus alleviating the need for anticoagulant therapy. Furthermore, the polymeric valves have the potential to overcome fatigue-related problems currently experienced by treated tissue valves.

Polymeric valves are generally made from a polyurethane-based material, which has demonstrated excellent blood compatibilty, hydrolytic stability, abrasion resistance, physical strength and flexure endurance.[14] Bernacca and colleagues examined the hydrodynamic behavior of biostable polyurethane valves, varying Young's modulus from 5 to 63.6 Mpa.[3] They demonstrated that the leaflet thickness has a more significant influence on the valve hydrodynamic function than the material modulus. Another study by Bernacca and colleagues showed that polymer valve durability is directly related to the leaflet thickness, with good durability achieved with a median leaflet thickness of approximately 150 μm.[1,2] Other studies with accelerated *in vitro* fatigue testing demonstrated that polymer valves with leaflet thicknesses of approximately 50 μm lasted less than 100 million cycles,[2] while leaflet thicknesses up to 200 μm lasted approximately 800 million cycles or 20 years.[1,2,16] More recent *in vivo* fatigue testing[5] found that the durability of polyurethane valves with leaflet thicknesses varying between 100 and 300 μm was between 600 million and 1 billion cycles, or 15.8–26 years.

Previous studies[4,10,13,30] indicated that the flow characteristics of these synthetic valves were comparable to those of bioprostheses. The flow distal of tri-leaflet synthetic valves was shown to have a relatively flat centralized profile with recirculation flow in the sinus cavity.[4,13] A maximum Reynolds shear stress (RSS) of 1447 dynes/cm^2 was

Address correspondence to Ajit P. Yoganathan, Professor, Associate Chair, School of Biomedical Engineering, Georgia Institute of Technology, 313 Ferst Drive, IBB Building, Room 2119, Atlanta, Georgia 30332-0535, USA. Electronic mail: ajit.yoganathan@bme.gatech.edu

recorded in one of the polyurethane valves.[4] Recent studies reported that the hemodynamic function of the implanted polymeric valves was comparable to that of the mechanical heart valves.[28,29]

Previous studies on the polymeric valves have focused on two main aspects: (1) animal studies, investigating the biostability of the various valve materials and the influence of valve designs on formation thrombus, and (2) hydrodynamic studies, investigating both the durability and flow characteristics of various valve designs and materials. Detailed flow information is required to determine how various valve designs affect the blood elements. However, previous *in vitro* experiments have not considered the small scale flow characteristics of the polymeric valves. The aim of this study is to examine in detail the flow structures inside, and in the immediate vicinity of, the tri-lealfet polymeric heart valve and to relate these to the thrombogenic potential of the valve.

METHODS

The two 23 mm tri-leaflet polymeric valves investigated in this study are shown in Fig. 1. The commissure region is defined as where the leaflets meet near the stent post. The gap channel, as shown in Fig. 1A, is located at the commissural region formed by the polyurethane leaflet wrapping around the stent structure. The coaptation region is the center region where the three leaflets meet and the high central region of the valve, as shown in Fig. 1, is located at the upper portion of the each leaflet near its trailing edge. The prototype A valve, shown in Fig. 1A, has a closed commissure design and a leaflet thickness of 80 μm, while the prototype B valve in Fig. 1B has an open commissure designs and a leaflet thickness of 120 μm. The figure shows the two valves at their free, or unstressed, state. A closed commissure design is characterized by the two adjacent leaflets being formed closer to each other near the stent region. On the other hand, in an open commissure design the adjacent leaflets do not come together near the stent but are well separated. The valves are prototype designs provided by AorTech Europe with leaflets manufactured from high silicone content polyurethane copolymer[3] (Elast-Eon^{TM}) and valve frames and stents machined from PEEK (Poly-etheretherketone). The polymeric valve was fabricated by dip-coating the PEEK frame with a thin layer of polyurethane leaflet.[16]

Laser Doppler Velocimetry

A fiber optic, three-component, coincident LDV system (Aerometrics Inc., CA) was used to acquire the 2D velocity field information inside and in the immediate vicinity of the polymeric tri-leaflet heart valves. In this system, a 4 W Argon-ion laser was coupled to a fiber drive unit, allowing color separation of the incoming primary beam. A two-component fiber optic transceiver probe with a 100 mm focal length lens was connected to the fiber drive. The resulting optics train produced an ellipsoidal probe volume with minor and major axes of approximately 21 μm and 140 μm, respectively.

Doppler signals were processed with Fast Fourier Transform based real-time signal analyzers (Aerometics Inc, CA). A software package provided by Aerometrics was used to acquire data and to control both the signal analyzers and the photomultiplier hardware. All measurements were conducted in the backscatter coincident mode in which a single probe acts as both the transmitter and receiver for the Doppler signals.

Measurement Locations

Fig. 2A shows the two orthogonal measurement planes downstream of the polymeric valves. Fig. 2B shows the locations of the six measurement stations along each plane, with distances referenced from the trailing edge of the leaflets. Fig. 3 shows the locations of the measurement planes both inside the valve and at the immediate

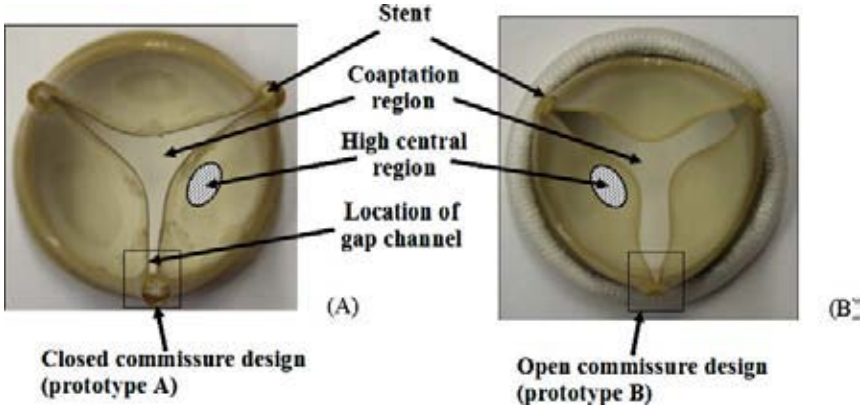

FIGURE 1. The two tri-leaflet polymeric heart valves investigated in this study. (A) Prototype A, with a closed commissural design and a leaflet thickness of 80 μm. (B) Prototype B, with an open commissural design and a leaflet thickness of 120 μm.

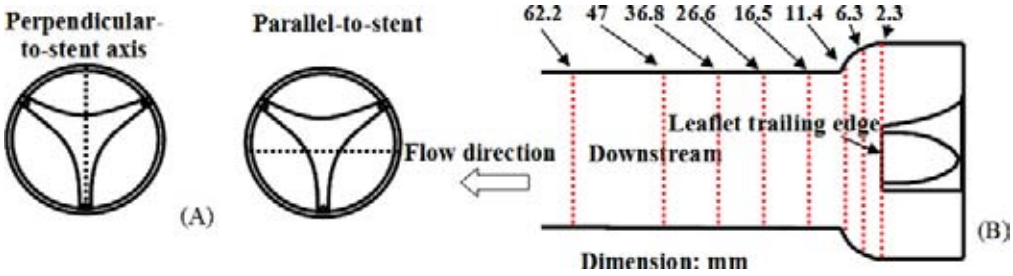

FIGURE 2. Measurement planes downstream of the prototype valves. (A) Data was acquired along two measurement planes downstream of the valve at eight different locations shown in (B). Distances are in mm referenced to the downstream leaflet edge.

downstream of the stent. The stent inflow region is indicated as the region along the inner side of each stent.

Flow Loop Setup

The valves were placed in a polycarbonate test section and mounted in the aortic position of the Georgia Tech left heart simulator. The flow loop, which was driven by a pulse generator, consisted of tubing, a mechanical valve at mitral position, a flow transducer, ventricular and aortic pressure transducers, a bulb pump, compliance, and resistance. Variation of the compliance and resistance sections of the loop allowed additional control in order to produce physiological flow and pressure waveforms. The heart rate was set at 70 beats/min, corresponding to an 860 ms cardiac cycle period, with a cardiac output of 5.0 L/min, a peak systolic flow rate of 25.0 L/min, a mean aortic pressure of 90-100 mmHg and a systolic flow phase duration of approximately 35% of the cardiac cycle time. The ventricular and aortic pressures were measured with pressure transducers (43-272, Baxter Healthcare Corporation, Irvine, CA) in conjunction with a CardioMed Amplifier (Medi-Stim AS, Norway). Flow rate was measured with a Transonic flow probe in conjunction with the CardioMed Amplifier. Fig. 4 shows the physiological flow waveform of the polymeric heart valves in the aortic position. A single cardiac cycle is characterized by two phases; the systolic phase and the diastolic phase. Systole is further subdivided into the acceleration, peak and deceleration phases.

The working fluid was a blood analog solution comprising 79% saturated aqueous sodium iodide, 20% glycerin, and 1% water by volume. The kinematic viscosity of 3.5 cSt matches that of blood at high shear rates. The fluid's refractive index, n, was adjusted by varying the amount of saturated aqueous sodium iodide to match those of the clear valve housing and polymeric leaflet ($n = 1.49$), thereby minimizing optical distortion. Silicon carbide particles (TSI Incorporated, MN) with a nominal diameter of 1.5 μm were used to seed the flow.

Data Reduction

Flow velocities were computed off-line using transit-time weighted averaging to eliminate velocity bias.[26] Velocities were phase-averaged within each 20 ms time windows (each cardiac cycle of 860 ms was divided into 43 time intervals) for subsequent analysis. Approximately 21,500 measurements were made at each location, an average of approximately 500 measurements within each 20 ms time window. This temporal resolution is long enough to ensure a valid statistical result in each time window and, at the same time, short enough for the data set within each time window to be considered quasi-steady. The maximum, or principal, values of the Reynolds shear stresses (RSS) were determined according to the formulation found in the literature and a detailed data analysis procedure can be found in earlier works.[8,9]

Leaflet Motion Study

The motion of the leaflets was acquired using Dual Camera Stereo Photogrammetry (DCSP), which incorporated two high-speed cameras (Basler a504k, Basler Vision Technologies, PA). An array of 30 markers, each approximately 1×1 mm^2, was applied to the entire leaflet surface

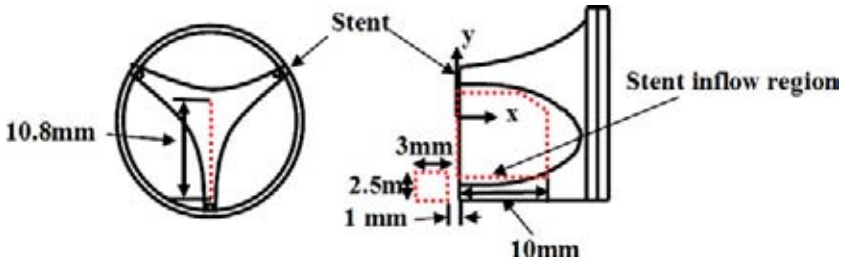

FIGURE 3. Measurement planes inside and immediately downstream of the stents.

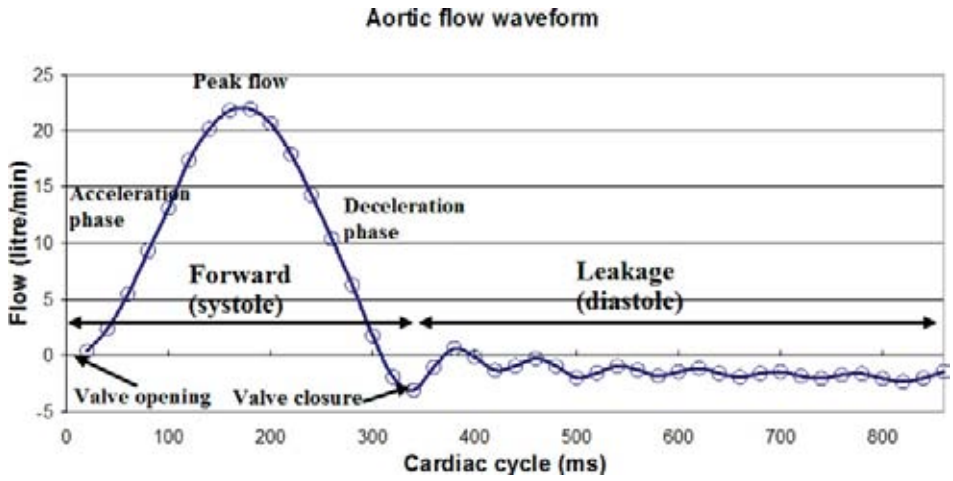

FIGURE 4. The aortic waveform generated by the pulsatile flow loop. The different phases of the cardiac cycle referred to in the text are labeled.

to allow detection of the leaflet by the camera. The leaflet position was recorded during the entire cardiac cycle at 500 frames per second with a resolution of 1280 × 1023 pixels (8 bit gray-scale). The angle of the cameras relative to each other was approximately 30°, centred on the valve, and they were connected to two synchronized EPIX high-speed framegrabber cards (PIXCI CL3SD imaging board, EPIX Inc., Buffalo Grove, IL) controlled by an imaging analysis software (EPIX, Inc, IL).

3D spatial coordinates of the dynamic leaflet surface were generated by tracking the position of the markers in a transient image sequence using an "in-house" MATLAB tracking program. The discrete data-points of the dynamic surface were interpolated into a smooth, contiguous surface using a Delaunay triangulation algorithm yielding a smooth 3D surface as described by David T. Sandwell.[20] In addition, a high-speed camera positioned 400 mm downstream of the polymeric valve captured the opening and closing motion of the leaflets through a viewing window generated by a dogleg extension downstream of the polycarbonate test section.

RESULTS

All of the results presented are based on phase averaged velocity fields. The flow characteristics of prototype A will be discussed first followed by those of the prototype B. For each prototype valve, the results will be in the following order: 1) downstream flow distribution; 2) measurements immediately downstream of the stent; and 3) measurements within the polymeric heart valve. The motion of the leaflets during the cardiac cycle, acquired with the high speed camera, will be presented after the velocity flow field results.

A summary of the maximum peak systole and diastole flow velocities for the two valves at various measurement planes is shown in Table 1.

Closed Commissure Valve with 80 μm Leaflet Thickness (Prototype A)

Flow Fields Downstream of the Valve

Figure 5A shows the flow field downstream of prototype A along the perpendicular-axis at peak systole. The peak systole velocity of 2.8 m/s occurred in the center orifice jet, 6.3 to 11.4 mm downstream of the valve, and coincided with a contraction of the core flow at the end of the sinus region, depicted schematically in Fig. 5B. The existence of the contraction of the center orifice jet, known as a vena contracta (defined as the contracted portion of a liquid jet at and near the orifice from which it issues), was evident in the LDV results. The strength of the center orifice jet decreased rapidly as the flow moved downstream and within the first 60 mm the velocity along the centerline of the jet

TABLE 1. Maximum velocity magnitudes inside and in the immediate vicinity of the polymeric heart valves during peak systole and diastole.

	Peak systolic phase			Diastolic phase		
	Downstream flow	Stent downstream	Inside valve	Downstream flow	Stent downstream	Inside valve
Prototype A	2.84 m/s (±0.013)	0.99 m/s (±0.126)	2.63 m/s (±0.039)	0.51 m/s (±0.069)	0.67 m/s (±0.178)	0.53 m/s (±0.086)
Prototype B	2.47 m/s (±0.063)	2.35 m/s (±0.071)	2.00 m/s (±0.068)	0.48 m/s (±0.165)	0.47 m/s (±0.079)	3.62 m/s (±0.252)

Note. All velocity measurements are phase averaged and their corresponding standard deviation are shown in parentheses.

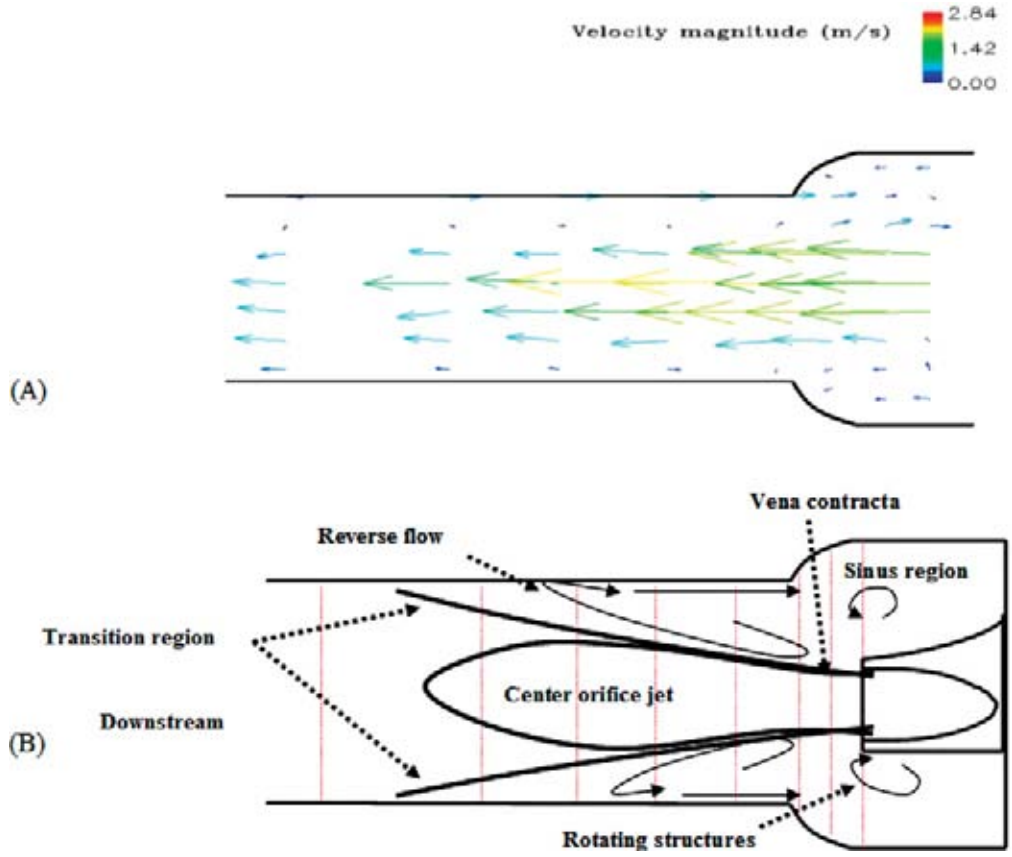

FIGURE 5. Velocity fields downstream of prototype A at peak systole. (A) Velocity vectors acquired along the perpendicular axis plane (Note: all velocity measurements are phase averaged). (B) Schematic of the flow field.

decreased by a factor of four. A separation zone extended approximately 62 mm downstream of the leaflet during peak systole flow phase; regions of reverse flow occurred along the chamber wall and a rotating flow structure was evident within the sinus region. During the diastolic phase, the fluid downstream of the valve was essentially stationary. A maximum RSS of approximately 8300 dynes/cm^2 was measured in the center orifice jet during peak systole and its location coincided with the vena contracta. The flow field along the parallel-axis measurement plane was similar to that measured along the perpendicular-axis.

Flow Downstream of the Stent

Detailed flow field measurements were acquired immediately downstream of the stent as the flow features of this region were not fully resolved in the downstream flow measurements. The flow fields in the region downstream of the stent at peak systole and diastole are shown in Figs. 6 and 7, respectively. At peak systole a forward jet with a maximum velocity of 0.98 m/s occurred through the gap channel at the commissural region. Regions of unsteady high velocity flow were observed near the stent during valve closure and the relative magnitude of the two largest vectors changed throughout diastole. A maximum RSS of approximately 1260 dynes/cm^2 was observed at the tip of the stent during the peak systole phase, while the shear stress levels away from the stent were very low, on the order of 30 to 100 dynes/cm^2. The maximum RSS during the diastolic phase was 200 dynes/cm^2.

Flow Inside the Valve

Figure 8 shows the velocity fields inside prototype A during peak systole. The forward flow near the inflow stent appeared to be directed upwards over the commissure at the leaflet trailing edge, and the maximum forward velocity of 2.6 m/s occurred at the trailing edge of the leaflet at peak systole. A region of low velocity flow occurred at the commissure and, as shown in Fig. 9, this low velocity region persisted during the deceleration phase. Fig. 10 shows the magnitude and location of the leakage flow within the valve during diastole. The peak leakage velocity of 0.5 m/s was observed directly upstream (relative to the forward flow direction) of the coaptation region, 3 to 4 mm from the leaflet edge. The flow inside the prototype A was unsteady at valve closure, but these fluctuations dissipated 140 to 160 ms after valve closure. The leakage flow

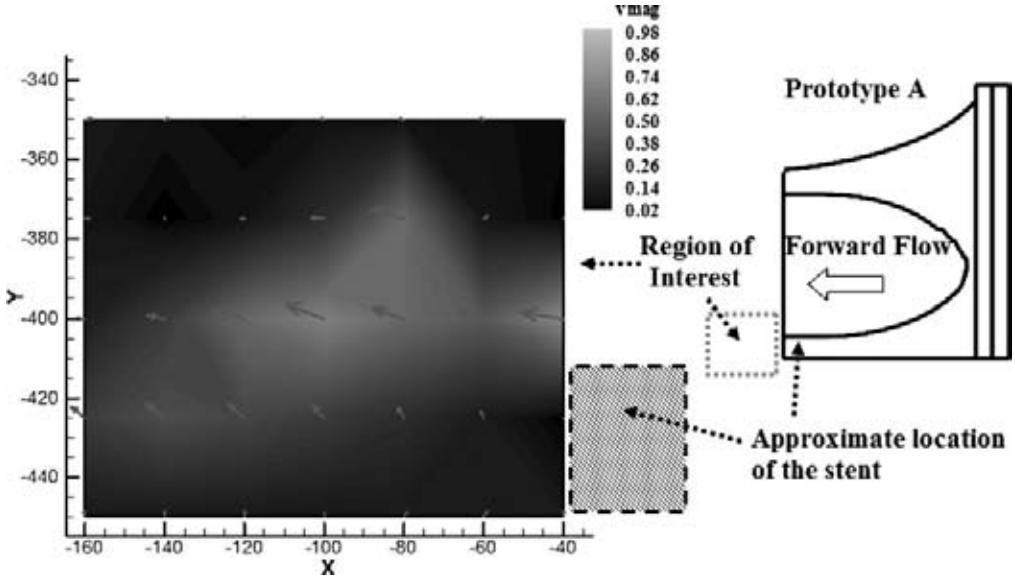

FIGURE 6. Velocity fields downstream of the stent of prototype A during peak systole. High velocity jet emanates from the gap channel at the commissural region.

oscillated in both magnitude and location during early diastole but became stable in location 220 ms after valve closure. The maximum RSS of 9000 dynes/cm^2 occurred along the trailing edge of the leaflet at the top side of the commissural region during peak systole flow. Examination of the shear stress distribution during systole phase indicated that high RSS values tended to occur near the edge of the valve and ranged between 2000 and 9000 dynes/cm^2. RSS levels were much lower during diastole, typically around 60 dynes/cm^2.

Opened Commissure Valve with 120-Micron Leaflet Thickness (Prototype B)

Flow Fields Downstream of the Valve

The flow fields downstream of prototype B during both systole and diastole, were similar to those described above for prototype A. The maximum flow velocity of 2.5 m/s was slightly higher than that found in prototype A, however the location of the peak velocity, as well as the locations of the separation and reattachment points, were the same for both

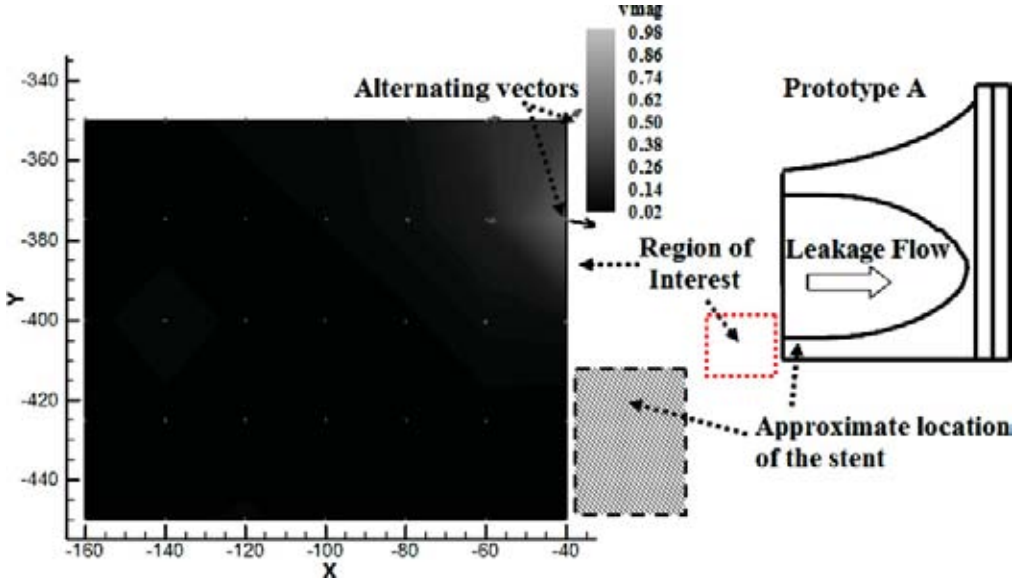

FIGURE 7. Velocity fields downstream of the stent of prototype A during early diastole. The leakage jet has a flow velocity of approximately 0.7 m/s.

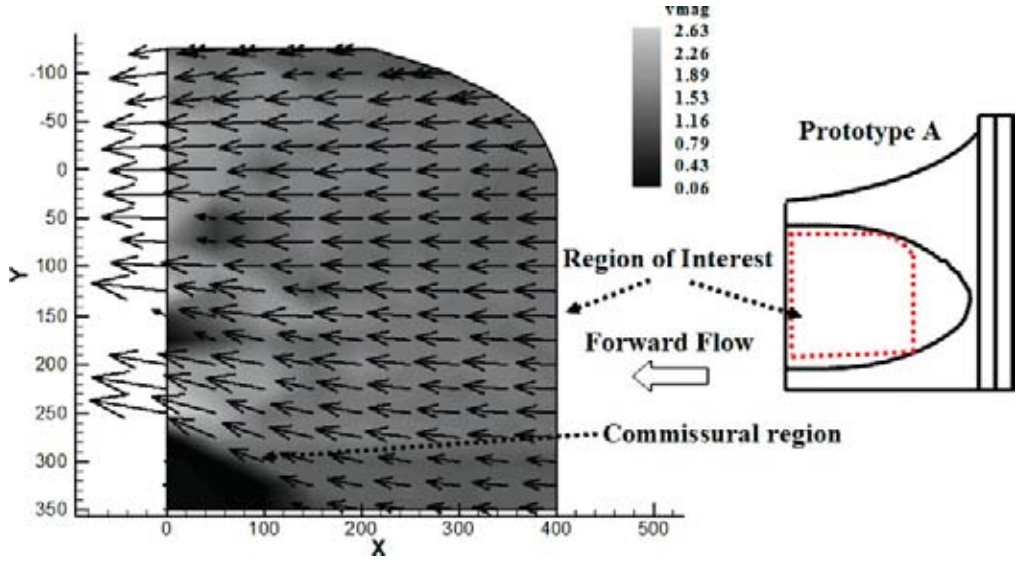

FIGURE 8. Velocity fields inside prototype A at peak systole. A peak forward velocity of 2.6 m/s was observed at the edge of the leaflet above the commissural region.

prototypes. The corresponding maximum RSS downstream of prototype B was 9000 dynes/cm^2 during the peak systole, while RSS values of approximately 100 dynes/cm^2 were observed throughout diastole.

Flow Downstream of the Stent

Fig. 11 shows the flow distribution downstream of the stent during peak systole. A maximum velocity of 2.3 m/s was observed immediately downstream of the stent during the peak systole phase. Examination of Fig. 11 during the forward flow period shows three distinct flow regions: a region of high velocity forward flow coming through the central valve orifice, a region of low velocity flow below the stent tip and a transition region between the high and low velocity flows. At the end of systole, the flow in the high velocity region slows down to approximately 0.5 m/s, but the general features of the flow regimes persisted. During early diastole, the flow downstream of the stent was unsteady, with leakage flow becoming established near the commissural region. The leakage flow, shown 320 ms after valve closure in Fig. 12, persisted throughout diastole with velocities of between 0.3 and 0.5 m/s. Maximum RSS levels of 6,000 dynes/cm^2 and 50 dynes/cm^2

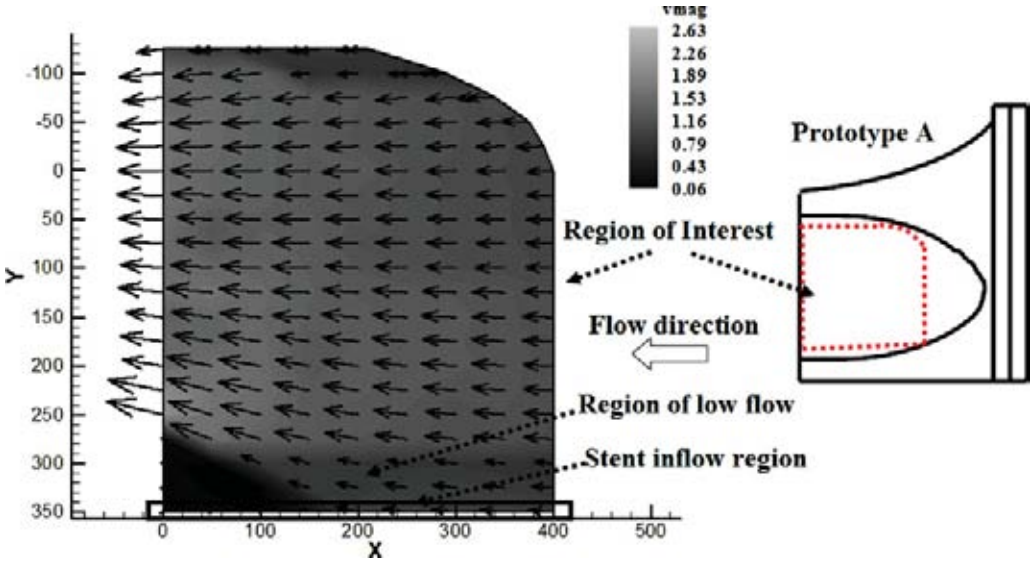

FIGURE 9. Velocity fields inside prototype A during deceleration phase. A region of low flow was evident at the stent inflow region.

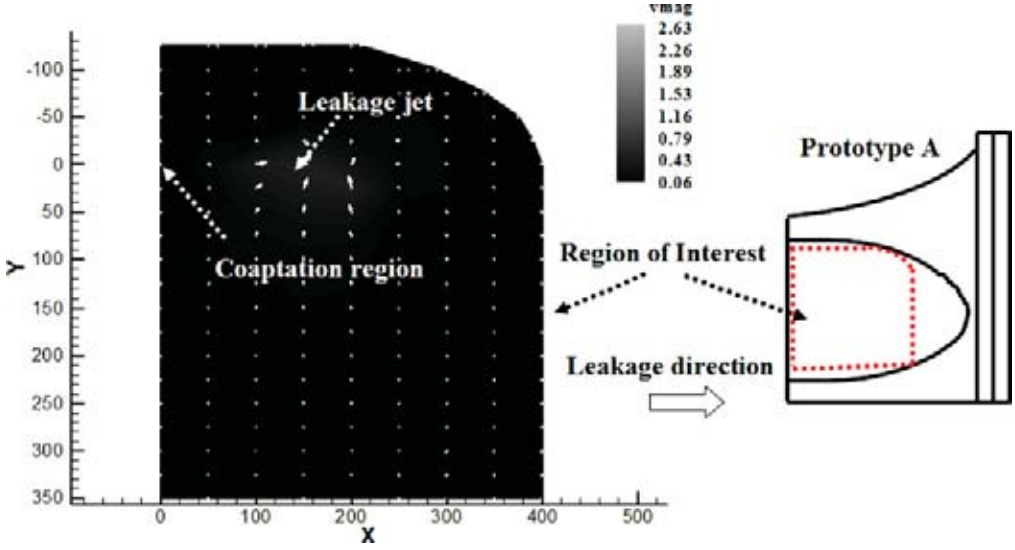

FIGURE 10. Velocity fields inside prototype A during diastole. The leakage jet is 3-4 mm from the coaptation region.

were observed immediately downstream of the stent tip during the peak systolic and diastolic phases, respectively. The location of the maximum shear stress did not correspond with that of the highest velocity, but occurred in the transition region between the high and low velocity flows.

Flow Inside the Valve

The flow inside prototype B, shown in Fig. 13 at peak systole, had a maximum forward flow velocity of 2.0 m/s at the edge of the leaflet. During peak systole, the flow field was relatively uniform and the low flow region that was shown in Fig. 9 for prototype A was not evident. After valve closure, the flow inside the valve was unsteady for 100 to 120 ms before stabilizing. A leakage jet appeared inside the valve approximately 160 ms after valve closure, oscillating in strength and position for 60 to 80 ms before stabilizing. The velocity magnitude of the leakage jet, shown 320 ms after valve closure in Fig. 14, appeared to originate approximately 2 mm upstream from the trailing edge of the leaflet and was significantly larger than the leakage jet observed in prototype A. The velocity of the leakage jet immediately following stabilization was 2.0 m/s. As the cycle continued, the jet gradually increased in both speed and size, reaching a maximum velocity of 3.6 m/s approximately 360 ms after valve closure. At this point, the leakage jet extended 5 mm from the leaflet edge,

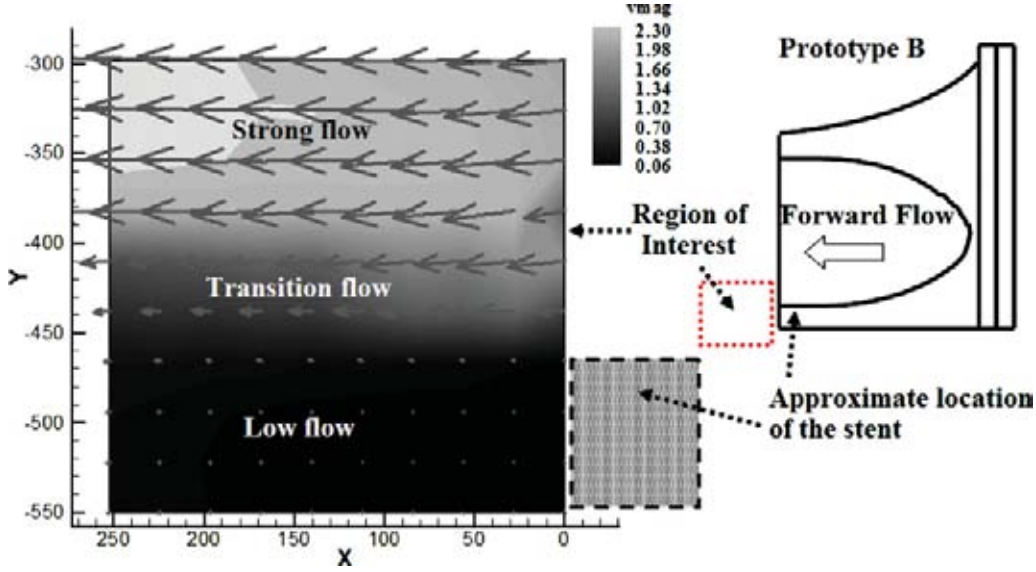

FIGURE 11. Velocity fields downstream of the stent of prototype B during peak systole.

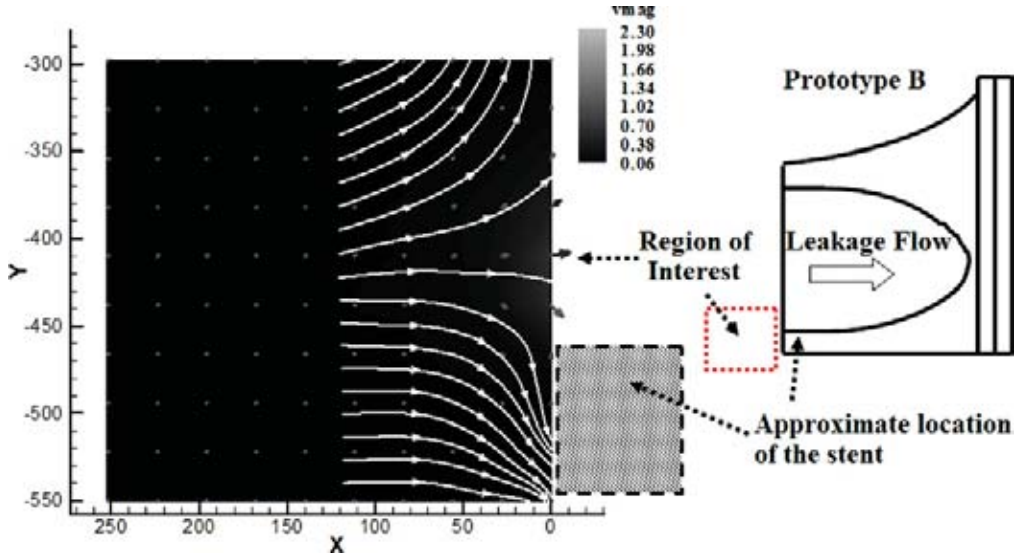

FIGURE 12. Velocity fields downstream of the stent of prototype B during diastole. Streamlines illustrate the presence of the stent tip below the gap channel.

occupying almost half of the measurement plane. The RSS values at all investigated locations inside the valve were less than 100 dynes/cm^2 during systole. The maximum RSS of approximately 13,000 dynes/cm^2 was observed in the leakage jet during diastole and is three orders of magnitude greater than the corresponding values for prototype A. The magnitude of RSS in the leakage jet during diastole ranged between 2,000 dynes/cm^2 220 ms after valve closure and 13,000 dynes/cm^2 360 ms after valve closure. The RSS values at other measurement locations inside the valve were generally less than 50 dynes/cm^2 during diastole.

High Speed Camera—Dynamic Motion of the Polymeric Valve

Figure 15 shows images of prototype A during peak systole and diastole respectively. Marker arrays along the edge and side of the leaflets were used to visualize the motion of the leaflets. Incomplete opening of the leaflets near the commissural region was evident during the systolic flow phase. After valve closure, the leaflets appeared to oscillate for 100 to 200 ms and leakage gaps were visible throughout diastole at both the commissural and coaptation regions. Fig. 16 shows the velocity of a single marker at the high

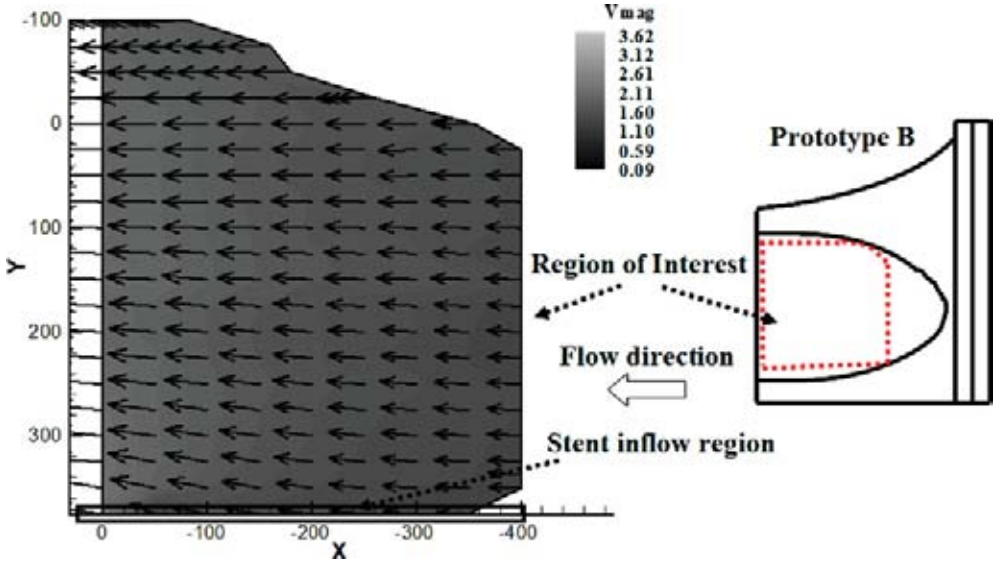

FIGURE 13. Velocity fields inside prototype B during peak systole.

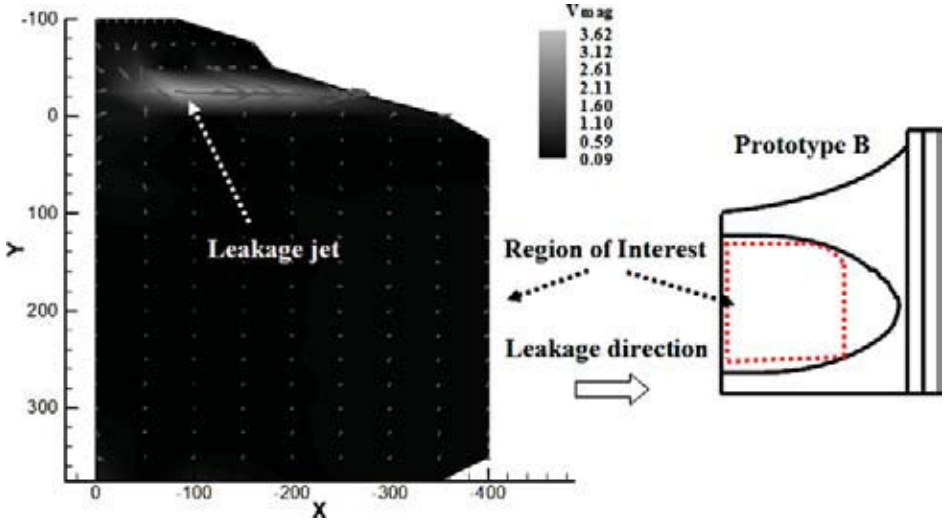

FIGURE 14. Velocity fields inside prototype B during diastole. A leakage jet was observed at the high central of the valve.

central region of the valve as a function of time; the opening and closing velocities of the leaflet at this location were 0.9 and 1.3 m/s, respectively. Oscillation, or 'bouncing,' of the valve was clearly evident following valve closure and persisted throughout diastole.

DISCUSSION

The discussion will be presented in the following sequence: 1) the similarities in the flow fields for the two prototype valves; 2) the differences in the flow fields between the two valves, in particular in the region of the stent tip and inside the valves; and 3) the influence of valve design on potential thrombus formation, including identification of regions inside the valve that could lead to platelet activation.

Similarity of the Flow Fields of the Two Polymeric Valves

The general characteristics of the flow downstream of both valves were similar to those observed for porcine and bovine tissue valves.[4,10,13,30] The flow distribution is characterized by a central orifice jet, shown schematically in Fig. 5B, with a region of flow separation occurring at the edge of the leaflets and flow reattachment further downstream. Both polymeric valves demonstrated center orifice jet flow velocities higher than 2.0 m/s during peak systole flow. These velocities occur several millimeters downstream from the valve edge in the vena contracta region. The beginning of the flow separation region corresponds to a sharp change in the cross-sectional area of the valve chamber as the flow moves into the sinus region.

The general features of the flow fields inside the two valves were similar, and in both cases, a maximum velocity of approximately 2.0 m/s occurred at the trailing edge of the leaflets. The valve leaflets were observed to 'bounce' for a period of 100 to 120 ms after valve closure. This oscillation can be attributed to the viscoelastic properties of the polymeric materials, which allow the leaflets and stents to flex under flow-induced loading. The fluid in the

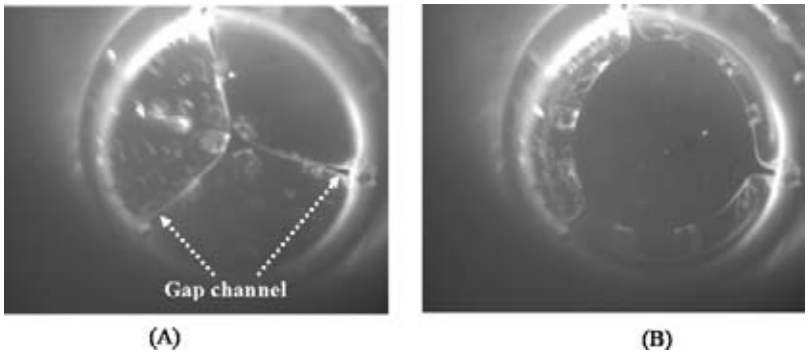

FIGURE 15. Images of the leaflets of prototype A captured by the high speed camera, (A) during systole. (B) Small orifices were observed at the coaptation region and the gap channel at the commissural region during diastole.

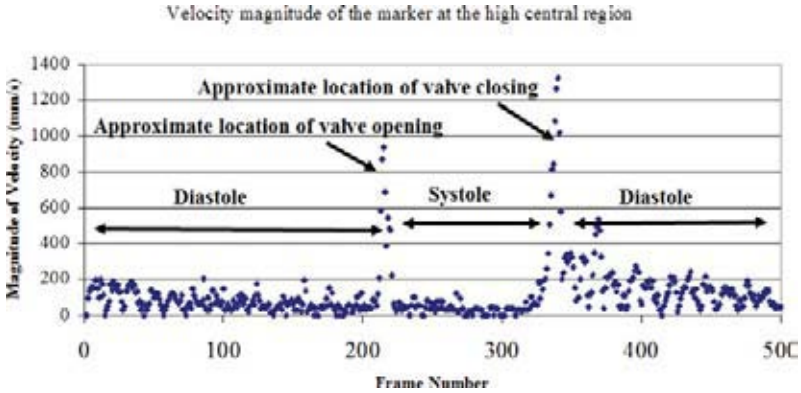

FIGURE 16. The displacement velocity of the leaflet at the high central region of prototype A during the cardiac cycle; demonstrating oscillation of the leaflet initiated at valve closure and persisting throughout diastole.

immediate vicinity of the leaflets and stents is affected by their motion, and the initial unsteadiness of the flow inside both valves and the oscillation of the leakage jet can be attributed to the bouncing of the valve during this period.

Differences in the Flow Fields of the Two Valves Designs

Figure 17 shows a schematic of the flow through the gap at the commissure next to the stent in prototype A and B during systole and diastole. During systole, a jet

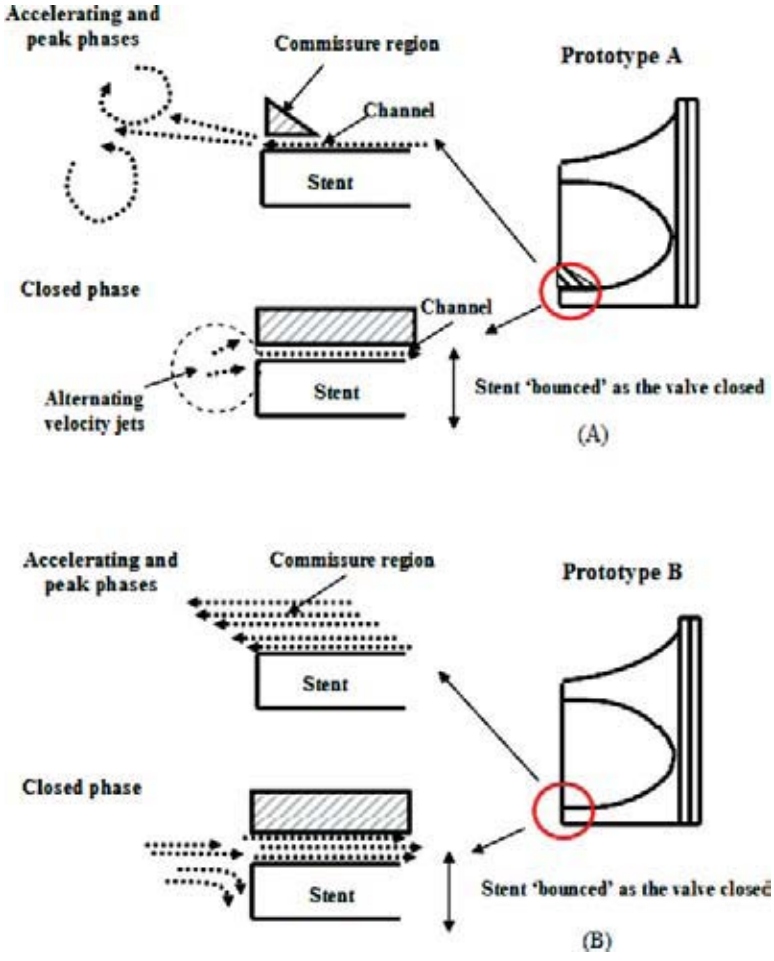

FIGURE 17. Schematic of the flow field at the stent during the acceleration and early diastolic phases, for prototypes A and B. The cross-hatched areas depict the regions where the adjacent leaflets at the commissure region come together.

with a maximum velocity of approximately 1.0 m/s flowed through the gap channel, giving rise to vortex structures downstream of the stent. Additionally, the location of the high velocity leakage flow during diastole corresponds to the gap channel. Unlike prototype A, prototype B has relatively unobstructed forward flow through the commissural region. As a result, the maximum forward flow velocity at the stent tip of prototype B (2.3 m/s) was more than double that of prototype A (1.0 m/s). During systole no gap channel was visible at the commissural region of prototype B; however, the flow field in Fig. 12 indicates that a commissural gap does in fact form during this period. The peak leakage flow velocity of 0.4 m/s at the stent region in prototype B was lower than the corresponding value of 0.7 m/s for prototype A. This can be attributed to a larger commissural gap in prototype B.

An area of stagnation, shown in Fig. 9, was evident at the commissural region of prototype A, throughout systole. This stagnation region gave rise to an area of low flow along the stent during the peak systole and deceleration phases. On the other hand, prototype B, does not generate a low flow region during systole. During the deceleration phase the flow velocity at the stent inflow region of prototype B (1.4 m/s) was double that of prototype A (0.8 m/s).

The flow velocities and size of the leakage jet in prototype B were much larger than in prototype A; the peak leakage jet velocity in prototype B of 3.6 m/s was more than four times that in prototype A, 0.8 m/s. This may be due to the thicker, and therefore stiffer prototype B leaflets, which could inhibit complete valve closure during diastole. Furthermore, the leakage jet in prototype B continued to increase in both magnitude and size after the initial stabilization period, nominally 220 ms after valve closure, while the corresponding prototype A leakage jet remained stable.

Relationship of Polymeric Valve Design to Thrombus Formation

It is generally accepted that the local activation of blood elements is related to both the magnitude of the shear stress and exposure time, and in turn these properties depend on the local fluid dynamics and geometry.[27] Regions of high shear stress could lead to platelet activation and the destruction of red blood cells.[17,22–24,27] Damaged and activated blood elements may also congregate in low flow regions, enhancing the formation and deposition of thrombi.

Research in recent years involving various mechanical and tissue heart valves has shown the importance of RSS calculation as a means of quantifying the damage of blood elements in valve prostheses.[6,7,11,15,18,19] These studies reported that hemolysis can occur for RSS values ranging from as low as 400 dyne/cm^2 to 5600 dyne/cm^2 with exposure time ranging from 10^2 to 10^{-4} s, while for platelet activation, the reported RSS threshold ranges between 100 dyne/cm^2 and 1000 dyne/cm^2, with exposure time varying from 10^2 to 10^{-2} s.

The results of the current experiments allow identification of three regions of high shear stress where the potential for platelet activation and hemolysis and subsequent thrombus formation is high: 1) the leakage jet inside the valve during diastole; 2) the trailing edge of the leaflet during systole; and 3) inside the center orifice jet during peak systole; where the duration of the high RSS levels in these regions was between 120 and 300 ms. The magnitude and duration of these shear stresses, ranging from 2000 dyne/cm^2 to more than 13,000 dyne/cm^2 are above the threshold values reported in the literature for the destruction of red blood cells and the activation of the platelets.

Animal studies involving sheep have shown that polymeric valves are prone to material degradation as a result of extrinsic calcification of the attached host biological material on the leaflet surface.[5,29] These studies found local fibrin deposits in the commissural region, which was attributed to the inefficient washout at the commissural region. Preliminary *in vivo* experiments involving prototype A and B designs also showed formation of thrombi along the commissure in the stent inflow region, and in the high central region of prototype B. Thrombus deposition along the stent inflow region of the prototype A were initially attributed to the inefficient washout at the closed commissural region. However, subsequent animal experiments with prototype B also showed similar thrombus formation along the stent region. Hence, the low flow region may not be the sole contributor to the observed thrombus.

Figure 18 shows the stream traces of the flow inside prototype B during diastole. The general flow feature inside the valve was that of flow 'splitting'; with a portion of the flow directed towards the center of the valve, i.e. towards the leakage jet, and the remainder of the flow moving towards the stent inflow region. This flow pattern was unsteady during early diastole, but stabilized 100 ms after valve closure and persisted throughout the diastolic phase. Similar flow features were observed in prototype A, but the pattern was less pronounced than in prototype B as a result of the lower velocity leakage jet. This observation was confirmed by the high speed camera results. The closing motion of prototype A, depicted in Fig. 19, indicates that the valve closes first at the lateral side of the leaflets (dotted arrows), forcing fluid towards the coaptation and stent inflow regions. In addition, the tracing of the marker array in Fig. 16, shows that small oscillation actually persist into late diastole. The closing dynamics of the valve and the persistence of the oscillations may give rise to the flow 'splitting' phenomenon, enhancing the transportation of activated blood elements towards the stent inflow and high central regions of the valve during diastole. The use of a thinner leaflet, despite the advantage of increase compliance and flexibility, may render the leaflets more prone to flow induced oscillations.

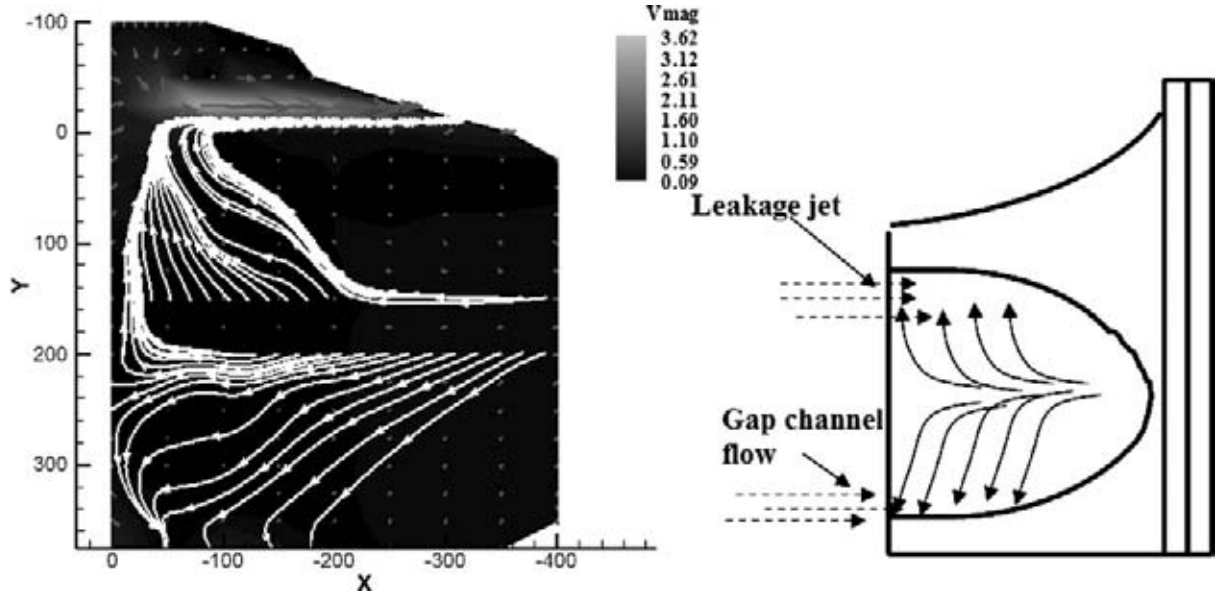

FIGURE 18. Stream traces of the flow inside prototype B during diastole.

Thrombus formation occurred in the high central region of prototype B but not in that the corresponding region of prototype A. It is likely that the higher shear stresses in the leakage jet of prototype B may be partially responsible for these clot buildups. Additionally, these thrombus depositions appear to correlate with the machining lines on prototype B. These machining lines, not evident on prototype A, were created during the fabrication process in which the polyurethane frames of the leaflet are mounted onto steel formers leaving indentations on the inflow side of the leaflets.[16] The surface topography at the high central region of prototype B in Fig. 20 clearly shows ridge pattern on the inner surface of prototype B. The peak ridge separation is approximately 100 μm and thrombus deposition is believed to have occurred at the troughs of the ridge pattern. The thinner leaflets of prototype A may render the valve more flexible hence enabling better valve closure during diastole, which would result in lower leakage jet velocities. On the other hand, the stiffer and thicker leaflets in prototype B may prevent complete valve closure resulting in higher leakage jet velocities. Coupled with a rougher inner leaflet surface, the thicker leaflets in prototype B likely led to the observed thrombus deposition in the high central region.

EXPERIMENTAL LIMITATIONS

A constraint to the current study was that only two different valve designs were investigated. Further work involving more valve designs would provide a much broader understanding of the effect of design parameters on the flow fields of polymeric valves. However, the authors believe

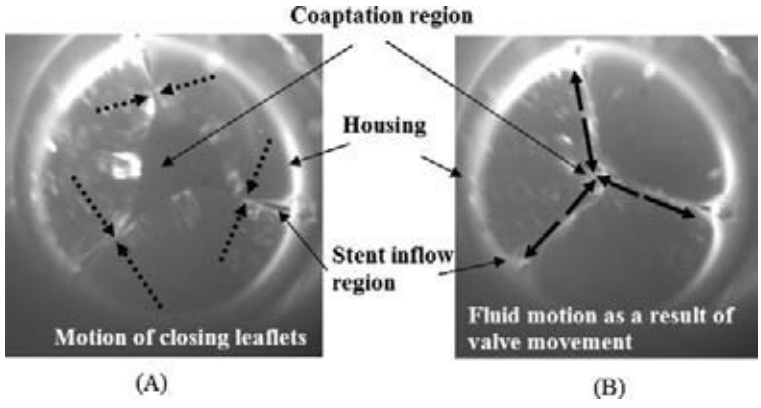

FIGURE 19. Images of prototype A illustrating the closing motion of the valve. (A) The valve closes first at the lateral side of the leaflets (dotted arrows). (B) Forcing fluid toward the coaptation and stent inflow regions (solid arrow).

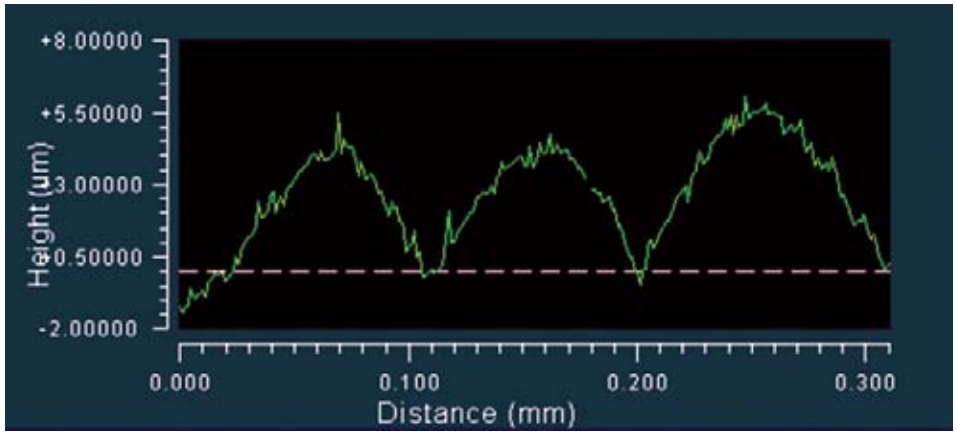

FIGURE 20. Surface topography of prototype B using white light interferometer. A ridge pattern was observed on the inner surface of leaflet at the high central region of prototype B.

that the current study set the ground work for further *in vitro* studies that will focus more on the hemodynamic aspects of polymeric heart valve design. Another limitation of the current study was that the LDV measurements were acquired in a 2D plane, thus any out of plane velocities are not represented. The low data rate sometimes encountered in the measurement contributed to the cyclic variation error for the turbulent shear stress. Lastly, in this study the prototype valves were mounted on rigid valve chambers. However, by ensuring that the waveforms obtained were compatible with that of the physiological conditions, the authors are confident that the *in vitro* set up could, to a very good approximation, mimic the flow dynamics of the *in vivo* conditions.

CONCLUSIONS

Hemolysis and platelet activation in artificial heart valves are primarily associated with regions of high shear stress, such as those in leakage jets and high velocity forward flow. Damaged or activated blood elements initiate a cascade resulting in thrombus formation, this may be further exacerbated by regions of low and recirculating flow. Therefore, it is imperative to highlight flow regions that may affect the thrombogenic potential of the prosthetic valve. The results of the present study indicate that commisural design and leaflet thickness can influence the thrombogenic potential of tri-leaflet polymeric valves. Specifically, the following regions of high shear stress and high velocity flow were identified: 1) the leakage jet inside the valve during diastole; 2) the trailing edge of the leaflet during peak forward flow; and 3) the center orifice jet downstream of the valve during peak forward flow. Low flow velocities were observed in the following regions include: 1) the inflow stent region in prototype A; 2) the closed commissural region of prototype A; and 3) the split flows inside both valve designs during diastole.

ACKNOWLEDGMENTS

This work was partially supported by a grant from the national Heart, Lung and Blood Institute (HL 720621). Prototype valves provided by Aortech, Inc.

REFERENCES

[1]Bernacca, G. M., T. G. Mackay, and D. J. Wheatley. *In vitro* function and durability of a polyurethane heart valve: Material considerations. *J. Heart Valve Dis.* 5(5):538–542, 1996.

[2]Bernacca, G. M., T. G. Mackay, M. J. Gulbransen, A. W. Donn, and D. J. Wheatley. Polyurethane heart valve durability: Effects of leaflet thickness and material. *Int. J. Artif. Organs* 20(6):327–331, 1997.

[3]Bernacca, G. M., B. O'Connor, D. F. Williams, and D. J. Wheatley. Hydrodynamic function of polyurethane prosthetic heart valves: Influences of Young's modulus and leaflet thickness. *Biomaterials* 23(1):45–50, 2002.

[4]Chandran, K. B., R. Fatemi, R. Schoephoerster, D. Wurzel, G. Hansen, G. Pantalos, L. S. Yu, and W. J. Kolff. *In vitro* comparison of velocity profiles and turbulent shear distal to polyurethane trileaflet and pericardial prosthetic valves. *Artif. Organs* 13(2):148–154, 1989.

[5]Daebritz, S. H., J. S. Sachweh, B. Hermanns, B. Fausten, A. Franke, J. Groetzner, B. Klosterhalfen, and B. J. Messmer. Introduction of a flexible polymeric heart valve prosthesis with special design for mitral position. *Circulation* 108 (Suppl 1):II134–II139, 2003.

[6]Ellis, J. T., T. M. Healy, A. A. Fontaine, R. Saxena, and A. P. Yoganathan. Velocity measurements and flow patterns within the hinge region of a medtronic parallel bileaflet mechanical valve with clear housing. *J. Heart Valve Dis.* 5(6):591–599, 1996.

[7]Ellis, J. T. and A. P. Yoganathan. A comparison of the hinge and near-hinge flow fields of the St Jude medical hemodynamic plus and regent bileaflet mechanical heart valves. *J. Thorac Cardiovasc. Surg.* 119(1):83–93, 2000.

[8]Ellis, J. T., B. R. Travis, and A. P. Yoganathan. An *in vitro* study of the hinge and near-field forward flow dynamics of the St. Jude Medical Regent bileaflet mechanical heart valve. *Ann. Biomed. Eng.* 28(5):524–532, 2000.

[9]Healy, T. M., J. T. Ellis, A. A. Fontaine, C. A. Jarrett, and A. P. Yoganathan. An automated method for analysis and

visualization of laser Doppler velocimetry data. *Ann. Biomed. Eng*. 25(2):335–343, 1997.

[10]Herold, M., H. B. Lo, H. Reul, H. Muckter, K. Taguchi, M. Giesiepen, G. Birkle, G. Hollweg, G. Rau, and B. J. Messmer. The Helmoltz-institute-tri-leaflet-polyurethane-heart valve prosthesis: Design, manufacturing and first *in-vitro* and *in vivo* results, In: Polyurethanes in Biomedical Engineering II, edited by H. E. A. Planck. Elsevier Science Publishers, 1987. pp. 231–268.

[11]Hung, T. C., R. M. Hochmuth, J. H. Joist, and S. P. Sutera. Shear-induced aggregation and lysis of platelets. *Trans. Am. Soc. Artif. Intern. Organs*. 22:285–291, 1976.

[12]Jamieson, W. R., L. H. Burr, W. N. Jr., Anderson, J. B. Chambers, J. P. Gams, and C. M. Dowd, Prosthesis-related complications: First-year annual rates. *J. Heart Valve Dis*. 11(6):758–763, 2002.

[13]Jansen, J., S. Willeke, B. Reiners, P. Harbott, H. Reul, H. B. Lo, S. Dabritz, C. Rosenbaum, A. Bitter, and K. Ziehe. Advances in design principle and fluid dynamics of a flexible polymeric heart valve. *ASAIO Trans*. 37(3):M451–M453, 1991.

[14]Lelah, M. D., and S. L. Cooper. Polyurethanes in Medicine. Boca Raton, Fla.: CRC Press, 1986, 225 p.

[15]Lu, P. C., H. C. Lai, and J. S. Liu. A reevaluation and discussion on the threshold limit for hemolysis in a turbulent shear flow. *J. Biomech*. 34(10):1361–1364, 2001.

[16]Mackay, T. G., D. J. Wheatley, G. M. Bernacca, A. C. Fisher, and C. S. Hindle. New polyurethane heart valve prosthesis: Design, manufacture and evaluation. *Biomaterials*. 17(19):1857–1863, 1996.

[17]Nemerson, Y., and V. T. Turitto. The effect of flow on hemostasis and thrombosis. *Thromb. Haemost*. 66(3):272–276, 1991.

[18]Ramstack, J. M., L. Zuckerman, and L. F. Mockros. Shear-induced activation of platelets. *J. Biomech*. 12(2):113–125, 1979.

[19]Sallam, A. M., and N. H. Hwang. Human red blood cell hemolysis in a turbulent shear flow: Contribution of Reynolds shear stresses. *Biorheology* 21(6):783–797, 1984.

[20]Sandwell, D. T. Biharmonic spline interpolation of GEOS-3 and SEASAT Altimeter data. *Geophys. Res. Lett*. (2):139–142, 1987.

[21]Simionescu, D. T., J. J. Lovekamp, and N. R. Vyavahare. Extracellular matrix degrading enzymes are active in porcine stentless aortic bioprosthetic heart valves. *J. Biomed. Mater. Res*. 66A(4):755–763, 2003.

[22]Slack, S. M., Y. Cui, and V. T. Turitto. The effects of flow on blood coagulation and thrombosis. *Thromb. Haemost*. 70(1):129–134, 1993.

[23]Slack, S. M., L. K. Jennings, and V. T. Turitto. Platelet size distribution measurements as indicators of shear stress-induced platelet aggregation. *Ann. Biomed. Eng*. 22(6):653–659, 1994.

[24]Slack, S. M., and V. T. Turitto. Flow chambers and their standardization for use in studies of thrombosis. On behalf of the subcommittee on rheology of the scientific and standardization committee of the ISTH. *Thromb. Haemost*. 72(5):777–781, 1994.

[25]Spina, M., F. Ortolani, A. E. Messlemani, A. Gandaglia, J. Bujan, N. Garcia-Honduvilla, I. Vesely, G. Gerosa, D. Casarotto, L. Petrelli, and M. Marchini. Isolation of intact aortic valve scaffolds for heart-valve bioprostheses: Extracellular matrix structure, prevention from calcification, and cell repopulation features. *J. Biomed. Mater. Res*. 67A(4):1338–1350, 2003.

[26]Tiederman, W. G., R. M. Privette, and W. M. Phillips. Cycle-to-cycle variation effects on turbulent shear stress measurment in pulsatile flows. *Exp. Fluids*. 6:265–272, 1988.

[27]Turitto, V. T., and C. L. Hall. Mechanical factors affecting hemostasis and thrombosis. *Thromb Res*. 92(6 Suppl 2):S25–S31, 1998.

[28]Wheatley, D. J., L. Raco, G. M. Bernacca, I. Sim, P. R. Belcher, and J. S. Boyd. Polyurethane: Material for the next generation of heart valve prostheses? *Eur. J. Cardiothorac. Surg*. 17(4):440–448, 2000.

[29]Wheatley, D. J., G. M. Bernacca, M. M. Tolland, B. O'Connor, J. Fisher, and D. F. Williams. Hydrodynamic function of a biostable polyurethane flexible heart valve after six months in sheep. *Int. J. Artif. Organs*. 24(2):95–101, 2001.

[30]Woo, Y. R., F. P. Williams, and A. P. Yoganathan. *In vitro* fluid dynamic characteristics of the abiomed trileaflet heart valve prosthesis. *J. Biomech. Eng*. 105(4):338–345, 1983.